J. Appl. Comput. Mech., 9(2) (2023) 487-497
DOI: 10.22055/jacm.2022.41405.3748

ISSN: 2383-4536
jacm.scu.ac.ir

Shahid Chamran University of Ahvaz

Journal of Applied and Computational Mechanics

Research Paper

The Impact of Marangoni Convection and Radiation on Flow of Ternary Nanofluid in a Porous Medium with Mass Transpiration

Thippaiah Maranna[1], Ulavathi S. Mahabaleshwar[2], Michael I. Kopp[3]

[1] Department of Mathematics, Shivagangotri, Davangere University, Davangere, India-577 007, Email: marannat4@gmail.com
[2] Department of Mathematics, Shivagangotri, Davangere University, Davangere, India-577 007, Email: u.s.m@davangereuniversity.ac.in
[3] Institute for Single Crystals, NAS Ukraine, Nauky Ave. 60, Kharkov 61001, Ukraine, Email: michaelkopp0165@gmail.com

Received July 20 2022; Revised October 23 2022; Accepted for publication October 24 2022.
Corresponding author: M.I. Kopp (michaelkopp0165@gmail.com)

Abstract. The current paper examines the impact of radiation and Marangoni convective boundary conditions on the flow of ternary hybrid nanofluids in a porous medium with mass transpiration effect on it. Estimated PDEs are converted to ODEs with consideration of the corresponding similarity transformations. The obtained non-dimensional reduced equations are solved by analytical process. A unique access based on the Laplace transform (LT) is used to find analytical solutions to the resulting equations. With the use of graphs, the exact solution may be investigated in the presence of many physical parameters such as solid volume fraction parameter, mass transpiration, porosity, radiation. The fluid flow contains three types of nanoparticles: spherical Silver (Ag), cylindrical SWCNT, and platelet graphene. Because of the shape composition of ternary hybrid nanoparticles, variation in concentrations is a primary factor of thermal performance. The shape of nanoparticles in ternary hybrid nanofluids has a major impact, and its application has the advantage of improving the cooling system's thermo-hydraulic performance.

Keywords: Marangoni convection, ternary hybrid nanofluid, mass transpiration, radiation, porosity.

1. Introduction

Recently, the role of nanofluids has substantially originated in various applications due to their properties being incomparably superior to those of other working fluids. The variety of nanoparticles is immersed in the working fluids to synthesize the nanofluids, and thus the optical, magnetic, thermal, mechanical, and electrical characteristics have been improved. Its relevance is found in micro reactors, solar collectors, microchannel heat sinks, enzymatic biosensors, bio separation systems, and micro-heat tubes. A steady fluid called a nanofluid is formed by suspending a particular type of nanoparticles in a basic fluid. But when there are two distinct types of nanoparticles, a hybrid nanofluid is developed and according to Shakya *et al.* [1], enhances the critical heat flux. The growing understanding of the development of nanofluids has resulted in the recognition of dimensions and forms of nanoparticles as a constant component affecting viscosity and thermal conductivity. Crane [2] and Wang [3] suggested the stretching sheet problem, which provides a diverse range of industrial services, as does incorporation of nanoparticles. Mahabaleshwar *et al.* [4] was one of the pioneer works on the investigation of outcomes of transferring heat in a viscoelastic liquid due to extending plate in the appearance of dissipation. Choi *et al.* [5] supported the notion of suspending nano regime particles in water-based fluids to increase the fluids' thermal conductivity in the beginning. Napolitano *et al.* [6-8] was the first study to examine the Marangoni boundary layer in their research, and also on the fields of identifications in mass and volume substances for non-Marangoni boundary layers which does contrarily depends about the configuration. On a thermo-solutal Marangoni permeable boundary with mass transpiration and heat source/sink, the impact of chemical radiation and heat penetration/formation of the viscous fluid flow was investigated by Mahabaleshwar *et al.* [9].

Recently, studies on the impact of ternary HNF on fluid flow and temperature distribution have begun. When it comes to energy exchanges, ternary hybrid nanofluid exceeds normal fluids, nanofluid, hybrid nanofluid, gasoline, and acetone. Hybrid nanofluids have a wide range of temperature-dependent effects, including freezing in high-temperature environments. Recently, Mahabaleshwar *et al.* [10-13] worked on Casson hybrid nanofluid, MHD flow micro polar fluid, and the MHD nanofluid through a penetrable and also stretching/shrinking surface, a horizontal surface having a radiated effect with mass transpiration. The incorporation of metal or metal oxide nanoparticles is a well-known technology for modifying the thermal conductivity of fluids. Due to their higher thermal conductivity over conventional heat transfer fluids, metal nanoparticles are the most beneficial. In modern research the suspension of the mixture of three different kinds of nanoparticles in a single base fluid is initiated which is called as ternary hybrid nanofluids. The thermal analysis of newly developed idea of ternary hybrid nanofluid with different shaped nanoparticles shows the promising heat transfer rate in many fields of sciences. Animasuan *et al.* [14] numerically

Published online: November 06 2022

explored the influence of an induced magnetic field and various shaped nanoparticles Ag, Al_2O_3, Al on flow, in addition to effect of a heat source/sink. Manjunatha *et al.* [15], conducted a theoretical analysis of convective heat transfer in a ternary nanofluid flowing across a stretching sheet. Effect of nanoparticle mixture ratio on the rheological behavior and thermophysical properties of Al2O3-TiO2-Cu/water ternary hybrid nanofluids was studied by Xuan *et al.* [16].

The ternary hybrid nanofluids thermal performance can be further enhanced compared to the conventional binary hybrid nanofluid by the inclusion of more nanoparticles, but this also means that its particle composition is more varied and its production is more complicated. Due to the complexity of preparation and comparative instability of ternary hybrid nanofluids, few studies have investigated the thermophysical properties of such fluids. Sahoo et al. [17] examined the impact of temperature and volume fraction on the Al_2O_3-CuO-TiO_2/W ternary hybrid nanofluid Comparing to the equivalent binary hybrid nanofluids, the 0.1 vol.% ternary hybrid nanofluid showed increases in viscosity of 55.41% and 17.25%. After that, a comparable investigation was carried out on the Al_2O_3-SiC-TiO_2/W ternary hybrid nanofluid [18]. A number of interesting numerical researches on the ideal fluid Marangoni boundary layers in varied configurations were interpolated through Refs. [19-20]. Manjunatha *et al.* [21] characterized the flow of a Cu-Al_2O_3-H_2O hybrid nanofluid with changing viscosity. The radially extended infinite gyrating disc with numerous slip effects that generates three-dimensional magneto stagnation-point flow of ternary hybrid nanofluid has been analyzed by Gupta *et al.* [22]. In the presence of mass transpiration (suction/injection) and radiation, a hybrid nanofluid (HNF) flows over a stretching/shrinking sheet was studied using an accurate analytical solution by Vishalakshi *et al.* [23]. Udawattha *et al.* [24] showed that the awareness of numerous facts about nanofluids comprising spherical nanoparticles has resulted from the relevance of nanofluid. The researchers discovered that increasing the volume proportion of nanoparticles enhances heat transfer. According to the research conducted by Ekiciler *et al.* [25], it was shown that due to a smaller thermal barrier layer, the nanoparticle in the form of the platelet exhibits the most significant heat transfer development. To the best of the authors' knowledge, a few studies have revealed remarkable thermo-physical properties of ternary hybrid nanofluid. As a consequence, the present study is aimed to examine the impact of the Marangoni convective boundary layer condition and radiation on a flow of ternary nanofluid in a porous medium with mass suction/injection effect. The present study is also based on the ternary nanofluid composed of Silver, SWCNTs, and Graphene nanoparticles in a H_2O as base fluid. By using the similarity transformation, a pair of nonlinear ordinary differential equations are constructed from the problem's governing equations. Analytical solutions are then determined by using the resulting similarity equations. The core of the proposed model is the analysis of the effects of different factors such as porosity parameter, solid volume fraction, mass suction/injection parameter, thermal radiation parameter on the flow and heat transfer behavior of the nanofluid. In addition, the effects of these factors on the flow of nanofluid regimes are sketched graphically. Thus, the novelty of the present problem includes the following aspects:

- The present study is aimed to investigate the flow of ternary nanofluid in a porous medium under influence of the Marangoni boundary condition, thermal radiation and mass suction/injection effects.
- Three various shaped nanoparticles are dispersed in the fluid flow viz, spherical Silver, cylindrical SWCNT and platelet graphene. Due to its shape configuration, variation in the concentrations of ternary hybrid nanoparticles acts as a major factor in thermal performance. Nanoparticle shape in ternary hybrid nanofluids affect significantly and its application has advantage in increasing the thermo-hydraulic performance of the cooling system.
- It is important to consider the thermal radiation in the present study as it plays a significant role in the industrial process and space technology involving high operating temperature.

2. Mathematical Modelling and Solution

In this paper, we consider a Marangoni boundary surface flow through permeable media in a water-based nanofluids containing three various nanoparticles in two continuous dimensions, namely Silver (Ag), Single-walled CNTs and Graphene (see Fig. 1). The basic fluid and particles are thermally balanced, the fluid is regarded inviscid, the flow is irrational, and the fluid is considered inviscid.

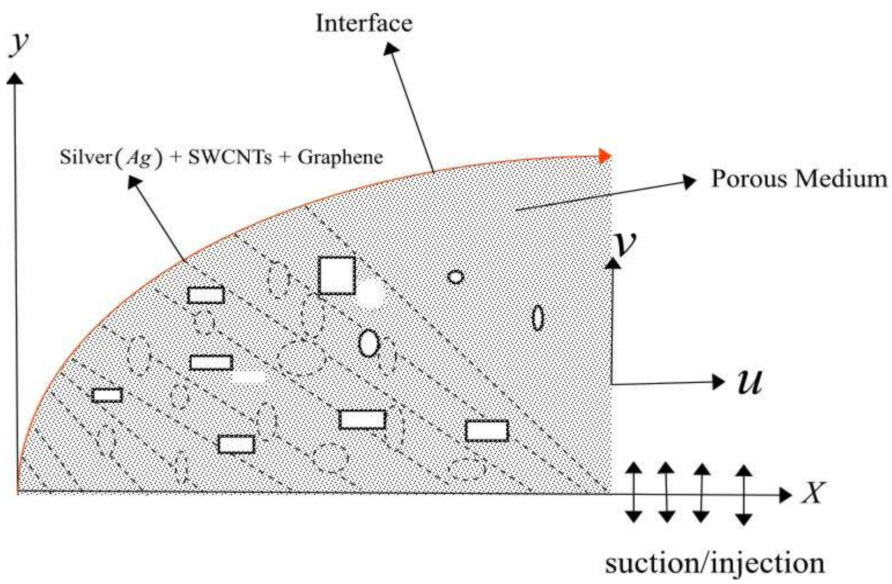

Fig. 1. Schematic representation of problem.

For the laminar boundary layer in the steady-state conditions, the governing equations of ternary nanofluid in Cartesian coordinates are stated as [27, 38]:

$$\frac{\partial u}{\partial x}+\frac{\partial v}{\partial y}=0\,, \tag{1}$$

$$u\frac{\partial u}{\partial x}+v\frac{\partial u}{\partial y}=\nu_{tnf}\frac{\partial^2 u}{\partial y^2}-\frac{\nu_{tnf}}{K}u\,, \tag{2}$$

$$u\frac{\partial T}{\partial x}+v\frac{\partial T}{\partial y}=\frac{\kappa_{tnf}}{\left(\rho C_p\right)_{tnf}}\frac{\partial^2 T}{\partial y^2}-\frac{1}{\left(\rho C_p\right)_{tnf}}\frac{\partial q_r}{\partial y}\,. \tag{3}$$

The last terms of Eqn. (2) and Eqn. (3) denote the porosity (porous medium) and thermal radiation, respectively. u and v represent the components of velocity in x and y directions, respectively, and the permeability is K.

The imposed boundary conditions are:

$$\begin{gathered} v=v_w\,,\quad T=T_\infty+ax^2\,,\quad \mu_{tnf}\frac{\partial u}{\partial y}=\frac{\partial \sigma}{\partial T}\frac{\partial T}{\partial y}\,,\ \text{at}\ \ y=0\,,\\ u=0\,,\quad T\to T_\infty\,,\ \text{at}\ \ y\to\infty\,. \end{gathered} \tag{4}$$

here μ_{tnf} is the dynamic viscosity of fluid, σ represents the surface tension parameter and v_w describes the mass suction/injection parameter, respectively. Next, we introduce the stream function with suitable similarity variables as follows:

$$\psi(\eta)=\xi_2 x f(\eta)\,,\quad \theta(\eta)=\frac{T-T_\infty}{ax^2}\,,\quad \eta=\xi_1 y\,, \tag{5a}$$

where T_∞ is the ambient temperature of the fluid. In the above equation, we have:

$$\xi_1=\frac{\sigma_0\gamma_a\rho_f}{\mu_f^{\,2}}\,,\quad \xi_2=\frac{\sigma_0\gamma_a\mu_f}{\rho_f^{\,2}}\,, \tag{5b}$$

with velocities in the following forms:

$$u=\xi_1\xi_2 x f'(\eta)\,,\quad v=-\xi_2 f(\eta) \tag{6}$$

The assumed surface tension with boundary condition (see [26-27]) is given by:

$$\sigma=\sigma_0[1-\gamma_T(T-T_\infty)]\,, \tag{7}$$

where σ_0 represents the surface tension at the interface and γ_T represents the rate at which the surface tension changes with temperature. The coefficient of surface tension for temperature is given by:

$$\gamma_T=-\frac{1}{\sigma_0}\frac{\partial \sigma}{\partial T}\bigg|_T\,. \tag{8}$$

The formula for radiative heat flux is obtained using Rosseland approximation, as stated in [28-31]:

$$q_r=-\frac{4\sigma^*}{3k^*}\frac{\partial T^4}{\partial y}\,. \tag{9}$$

The temperature of flow changes as the continuous functions of T^4. As a result, we can obtain it by expanding the Taylor series up to the term T^4 about T by eliminating the higher order terms as:

$$T^4\cong 4T_\infty^3 T-3T_\infty^4\,. \tag{10}$$

Eqn. (9) and Eqn. (10) gives:

$$q_r=-\frac{16\sigma^* T_\infty^3}{3k^*}\frac{\partial T}{\partial y}\,, \tag{11}$$

here σ^* is the constant of Stefan-Boltzmann, whereas k^* is the coefficient of mean absorption. Obviously in the view of similarity transformation, the continuity equation is satisfied. According to basic Eqns. (2) and (3), the following is transformed along with the boundary conditions. The dimensional form of ODEs are as follows:

$$\frac{A_1}{\phi}\frac{\partial^3 f}{\partial \eta^3}+A_2\left\{f(\eta)\frac{\partial^2 f}{\partial \eta^2}-\left(\frac{\partial f}{\partial \eta}\right)^2\right\}-\frac{A_1}{\phi}K_p\frac{\partial f}{\partial \eta}=0\,. \tag{12}$$

The energy equation becomes:

$$\left(A_3+Nr\right)\frac{\partial^2 \theta}{\partial \eta^2}+A_4\Pr\left\{f(n)\frac{\partial \theta}{\partial \eta}-2\frac{\partial f}{\partial \eta}\theta(\eta)\right\}=0\,, \tag{13}$$

Table 1. The thermo-physical properties of ternary hybrid nanofluids (see [32, 33]).

Nanoparticles/base fluid	ρ (Kg/m^3)	κ (W/mK)	C_p (J/KgK)	Shapes
Water (H_2O)	997.1	0.613	4180	Pr = 6.1723
Silver (Ag)	163.46	163.16	235	spherical
Single-walled CNTs	103.70	103.42	425	cylindrical
Graphene	73.46	74.38	790	platelet

where $A_2 = \rho_{tnf} / \rho_f$, and $K_p = \mu_f / \rho_f K \xi_1 \xi_2$ is the porosity parameter. $A_3 = \kappa_{tnf} / \phi \kappa_f$, $A_4 = (\rho C_p)_{tnf} / (\rho C_p)_f$, and $\Pr = \upsilon_f (\rho C_p)_f / \kappa_f$ is the Prandtl number, $Nr = 16\sigma^* T_\infty^3 / 3(\rho C_p)_f \upsilon_f k^*$ is the thermal radiation parameter. The surface velocity can then be intended by using

$$u_w = \left[\frac{(\sigma_0 \gamma_a)^2}{\rho_f \mu_f}\right]^{\frac{1}{3}} \times \left(\frac{\partial f}{\partial \eta}\right)_{\eta=0} . \tag{14}$$

In order to understand the water-based ternary nanofluids dynamics, the viscosity in a dynamic state is denoted as μ_{tnf}, thermal conductivity is to be κ_{tnf}, ρ_{tnf} is the density and heat capacitance is represented by $(\rho C_p)_{tnf}$. The imposed boundary conditions have been modified as:

$$\left(\frac{\partial^2 f}{\partial \eta^2}\right)_{\eta=0} = -2\frac{\phi}{A_1}, \quad f(0) = f_w, \quad \left(\frac{\partial f}{\partial \eta}\right)_{\eta=0} = 0, \quad \theta(0) = 1, \quad \theta(\infty) = 0 . \tag{15}$$

The quantities of nanofluids are defined as follows (see [34-37]):

$$\begin{gathered}
\mu_{tnf} = \frac{\mu_{nf_1}\phi_1 + \mu_{nf_2}\phi_2 + \mu_{nf_3}\phi_3}{\phi}, \\
\rho_{tnf} = (1 - \phi_1 - \phi_2 - \phi_3)\rho_f + \phi_1 \rho_{sp_1} + \phi_2 \rho_{sp_2} + \phi_3 \rho_{sp_3}, \\
\kappa_{tnf} = \frac{\kappa_{nf_1}\phi_1 + \kappa_{nf_2}\phi_2 + \kappa_{nf_3}\phi_3}{\phi}, \\
(\rho C_p)_{tnf} = (1 - \phi_1 - \phi_2 - \phi_3)(\rho C_p)_f + \phi_1(\rho C_p)_{sp_1} + \phi_2(\rho C_p)_{sp_2} + \phi_3(\rho C_p)_{sp_3}, \\
\phi = \phi_1 + \phi_2 + \phi_3,
\end{gathered} \tag{16}$$

here ϕ is the volume fraction of the ternary nanofluid and ϕ_1, ϕ_2, together with ϕ_3 are the corresponding volume fraction of the spherical, cylindrical and platelet nanoparticles respectively.

The spherical nanoparticle quantities are:

$$\begin{gathered}
\frac{\mu_{nf_1}}{\mu_f} = 1 + 2.5\phi + 6.2\phi^2, \\
\frac{\kappa_{nf_1}}{\kappa_f} = \frac{\kappa_{sp_1} + 2\kappa_f - 2\phi(\kappa_f - \kappa_{sp_1})}{\kappa_{sp_1} + 2\kappa_f + \phi(\kappa_f - \kappa_{sp_1})} .
\end{gathered} \tag{17}$$

The cylindrical nanoparticle quantities are:

$$\begin{gathered}
\frac{\mu_{nf_2}}{\mu_f} = 1 + 13.5\phi + 904.4\phi^2, \\
\frac{\kappa_{nf_2}}{\kappa_f} = \frac{\kappa_{sp_2} + 3.9\kappa_f - 3.9\phi(\kappa_f - \kappa_{sp_2})}{\kappa_{sp_2} + 3.9\kappa_f + \phi(\kappa_f - \kappa_{sp_2})} .
\end{gathered} \tag{18}$$

The platelet nanoparticle quantities are:

$$\begin{gathered}
\frac{\mu_{nf_3}}{\mu_f} = 1 + 37.1\phi + 612.2\phi^2, \\
\frac{\kappa_{nf_3}}{\kappa_f} = \frac{\kappa_{sp_3} + 4.7\kappa_f - 4.7\phi(\kappa_f - \kappa_{sp_3})}{\kappa_{sp_3} + 4.7\kappa_f + \phi(\kappa_f - \kappa_{sp_3})} .
\end{gathered} \tag{19}$$

3. Analytical Solutions for Momentum

3.1 Analytical solution of *f(h)*

The assumed analytical solutions of the momentum Eqn. (12) with respect to the boundary condition in Eqn. [15], is given by [27]:

$$f(\eta) = c_1 + c_2 \exp(-\beta\eta), \tag{20}$$

here (see [22]):

$$c_1 = f_w - c_2\,,\quad c_2 = \frac{-2\phi}{\beta^2 A_1} \tag{21}$$

Substituting Eqn. (20) and Eqn. (21) into Eqn. (12), we get the value of β :

$$\frac{A_1}{\phi}\beta^3 - A_2 f_w \beta^2 - \frac{A_1}{\phi}K_p\beta - 2\frac{\phi}{A_1} = 0\,, \tag{22}$$

where the positive resultant value is simply taken into account to arrive at the physical solution. In the next section, we will discuss the analytical solution of temperature equation.

3.2 Analytical solution of $\theta(\eta)$ using Laplace transformation

In relation to the benefits of Laplace transformation discussed in the previous section and to solve the temperature Eqn. (13), we use this approach, and its proper condition (15). Another approach to the solution can be conducted using a variable transformation technique. In order to solve Eqn. (13), a new variable $t = -\exp(-\beta\eta)$ is introduced and substituted in Eqn. (13), one obtains:

$$t\frac{\partial^2\theta}{\partial t^2} + (n - mt)\frac{\partial\theta}{\partial t} + 2m\theta(t) = 0\,, \tag{23}$$

where

$$m = 2\frac{\tau\phi}{\beta^2 A_1}\,,\quad n = 1 - \frac{\tau}{\beta}\left(f_w + \frac{2\phi}{\beta^2 A_1}\right), \tag{24}$$

and

$$\tau = \frac{A_4 \Pr}{(A_3 + Nr)} \tag{25}$$

subject to the accompanying set of boundary conditions:

$$\theta\left(0^-\right) = 0\,,\quad \theta(-1) = 1\,. \tag{25a}$$

Now, by introducing the Laplace transformation on both sides of Eqn. (23), we have

$$s(m - s)\frac{\partial\Theta}{\partial s} + \{(n-2)s + 3m\}\Theta(s) = 0\,, \tag{26}$$

here $\Theta(s)$ is the Laplace transformation of $\theta(t)$, by integrating Eqn. (26), we get

$$\Theta(s) = \frac{c}{s^3(s-m)^{-(n+1)}}\,, \tag{27}$$

where c is an integration constant as to be determined later, now applying the inverse Laplace transform on Eqn. (27) leads to:

$$\theta(t) = \frac{ct^2 t^{-(n+2)} e^{mt}}{2\Gamma(-(n+1))}\,. \tag{28}$$

Now, using the convolution theorem defined by

$$L^{-1}[\phi(s), \psi(s)] = \phi(t) * \psi(t) = \int_0^t \psi(w)\phi(t-w)dw\,, \tag{29}$$

where * denotes the convolution property. In addition, we have $L^{-1}\{\phi(s)\} = \phi(t)$ and $L^{-1}\{\Psi(s)\} = \Psi(t)$, then Eqn. (29) becomes:

$$\theta(t) = \frac{c}{2\Gamma(-(n+1))}\int_0^t \frac{(t-w)^2 e^{mw}}{w^{n+2}}dw\,,\quad n < -1 \tag{30}$$

by putting the modified boundary conditions into action, i.e. $\theta(0) = 0$ is spontaneously fulfilled. Moreover, another boundary condition $\theta(-1) = 1$ gives c as:

$$c = -\frac{2\Gamma(-(n+1))}{\int_{-1}^{0}(1+w)^2 w^{-n-2} e^{mw} dw}\,. \tag{31}$$

Consequently, $\theta(t)$ will be presented in exact arrangement

$$\theta(t) = \frac{\int_0^t (t-w)^2 w^{-n-2} e^{mw} dw}{\int_1^0 (1+w)^2 w^{-n-2} e^{mw} dw}\,. \tag{32}$$

Relating to the generalized incomplete gamma function, we get the following exact solution by integrating Eqn. (32):

$$\theta(t)=\frac{m^2t^2\Gamma(-n-1,0,-mt)+2mt\Gamma(-n,0,-mt)+\Gamma(-n+1,0,-mt)}{m^2\Gamma(-n-1,0,m)-2m\Gamma(-n,0,m)+\Gamma(-n,0,m)}. \tag{33}$$

Finally, it will be stated as follows in relation to η :

$$\theta(\eta)=\frac{m^2e^{-2m\eta}\Gamma\left(-n-1,0,me^{-\beta\eta}\right)-2me^{-\beta\eta}\Gamma\left(-n,0,me^{-\beta\eta}\right)+\Gamma\left(-n+1,0,me^{-\beta\eta}\right)}{m^2\Gamma(-n-1,0,m)-2m\Gamma(-n,0,m)+\Gamma(-n+1,0,m)}. \tag{34}$$

In this part, it was determined that utilizing as a problem-solving tool, the Laplace transform produces a simpler unique attributes, but manipulating the alternative approaches, generates more complex special functions.

4. Results and Discussion

In a porous media with mass transpiration, we investigate the effects of radiation and Marangoni convective boundary conditions on the flow of various ternary hybrid nanofluids. The analytical approach is used to solve the dimensionless ordinary differential equations (12)-(15), as described in the previous section. Our findings are interpreted using Graphs in this section. Figures 2(a)-(c) display the velocity profile against the variation of mass transpiration parameter and the porosity parameter, and volume friction was highlighted. It has been revealed that by enhancing the values of ϕ, velocities diminish considerably. As a result, as the distance from the boundary rises, the momentum boundary layer's thickness reduces also approaches to zero. Thermal diffusivity increases as the thermal conductivity increases. As a consequence, changing the values of ϕ affect the thickness of the boundary layer.

Figures 3(a)-(c) and Figures 4(a)-(c) show the result of porosity against velocity profile and temperature distribution. It should be observed that as porosity values grows, indicating an enhances in permeability particles, mobility improves in both types of nanoparticles and is similar at suction injection and no permeability instances. This is, of course, agreed with the physical view. It should be noted here that, for $K \le 0.1$, when suction and injection instances are used, the present three types of nanoparticles have essentially identical thermal performance.

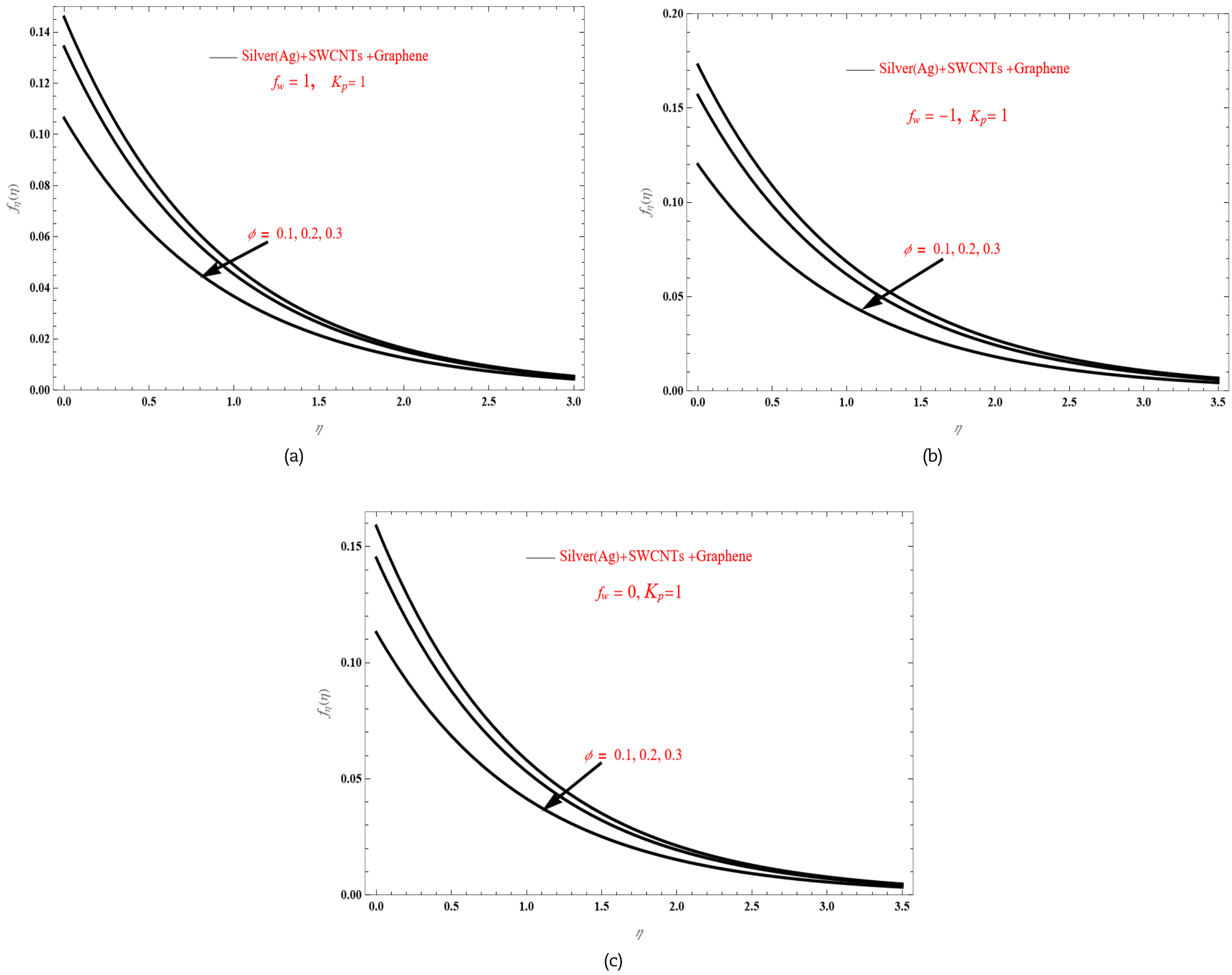

Fig. 2. (a) Velocity profile $f'(\eta)$ for variation of ϕ with K_p =1 and f_w = 1 (b) Velocity profile $f'(\eta)$ for variation of ϕ with K_p =1 and f_w = -1 (c) Velocity profile $f'(\eta)$ for variation of ϕ with K_p =1 and f_w =0.

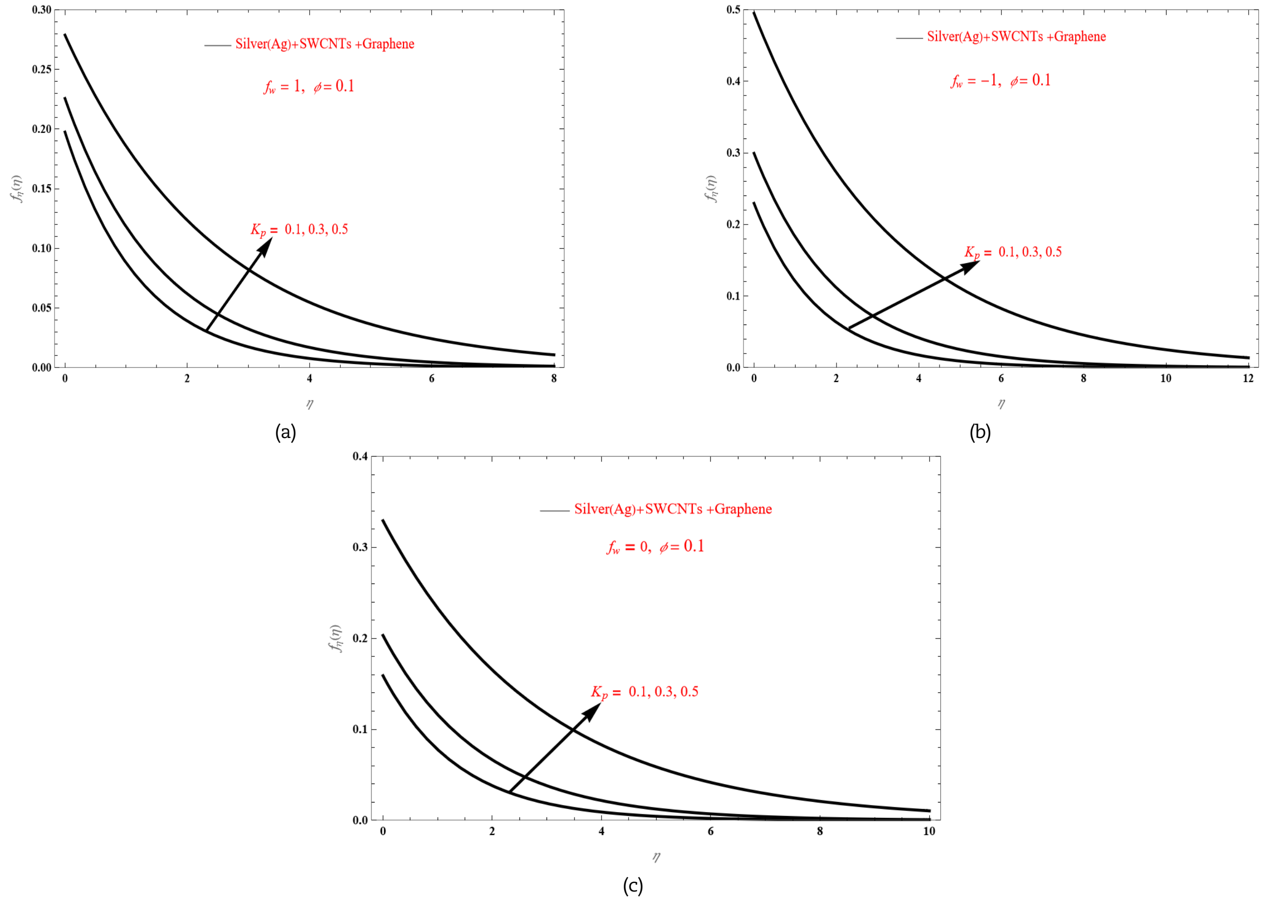

Fig. 3. (a) Axial velocity for variation of K_p with f_w =1 and ϕ = 0.1 (b) Axial velocity for variation of K_p with f_w = -1 and ϕ = 0.1 (c) Axial velocity for variation of K_p with f_w = 0 and ϕ = 0.1.

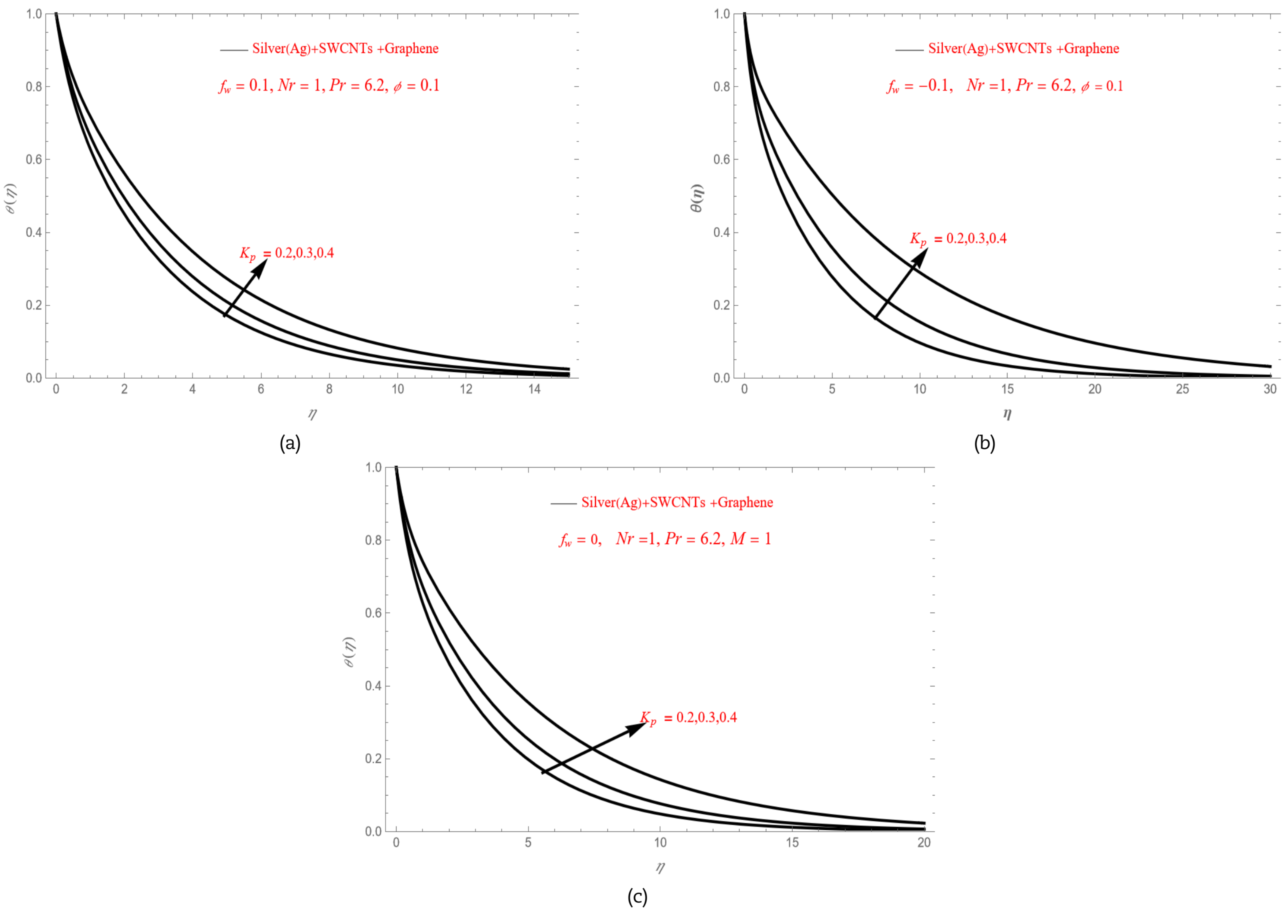

Fig. 4. (a) Temperature distribution for variation of k_p with f_w =0.1 and Nr =1 (b) Temperature distribution for variation of K_p with f_w = -0.1 and Nr =1 (c) Temperature distribution for variation of K_p with f_w = 0 and Nr =1.

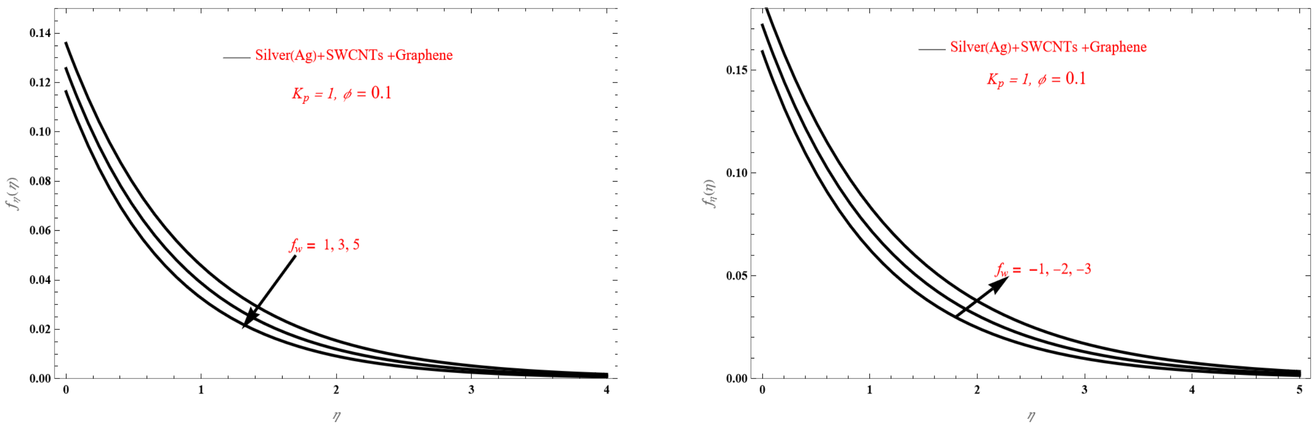

(a) (b)

Fig. 5. (a) Axial velocity for variation of f_w with K_p=1 and ϕ = 0.1 (b) Axial velocity for variation of f_w with K_p =1 and ϕ = 0.1.

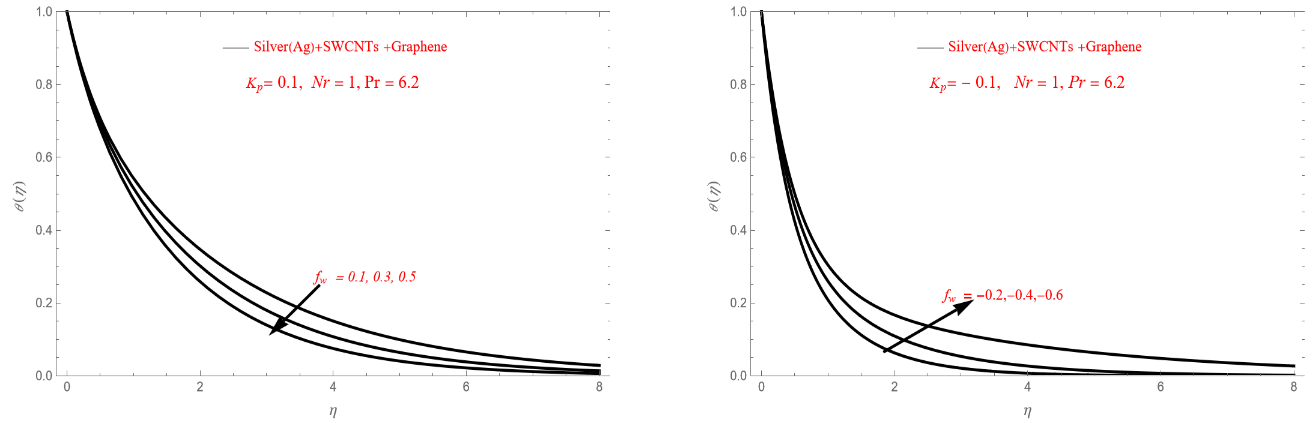

(a) (b)

Fig. 6. (a) Temperature distribution for variation of f_w with values of Nr = 1 and K_p =0.1 (b) Temperature profile for variation of f_w with values of Nr = 1 and K_p = -0.1.

Figure 5(a)-(b) and Figure 6(a)-(b) describes the respectively, velocity and temperature variations. It has been demonstrated that exerting fluid suction reduces in relation to fluid temperature and the heat transfer layer, as well as flow rates and hence the hydraulic boundary layer thickness. Fluid injection, on the other hand, has the reverse effect, enhancing fluid velocity and temperature. At different conditions namely, suction/injection case the three nanoparticles have identical temperature and velocity variations.

The radiation parameter estimates the relevance of thermal radiation transmission in comparison to convective heat transfer. Thermal characteristics enhance of radiation parameter increases for all three nanoparticles tested, as well as mass transpiration parameter scenarios studied, as shown in Figures 7(a)-(c), and in Figure 7(a) it is observed that density of all these three nanoparticles are identical. Therefore, the profiles show that thermal radiation has a greater impact on increasing the nanofluid temperature. Physically, strengthening radiative features stimulate the molecule mobility within the fluid, resulting in heat energy being converted through frequent collisions between nanoparticles when the surface wall is at both case of suction($f_w > 0$) or injection ($f_w < 0$) and no permeability, and both types of nanoparticles.

Figures 8(a)-(c) show how the percentage of volume influences the temperature curves, respectively. As the volume fraction of nanoparticles grows, the temperature within the nanofluid rises, generating more area for higher heat conduction. This raises the temperature of the nanofluid, as illustrated. This enhances heat absorption and helps the appliance to maintain an acceptable temperature and a long life. The fluid with them in their travel direction and thus the velocity of the fluid flow rises, as shown in this figure. All nanoparticles have nearly same temperature distribution.

5. Conclusion

The aim of the present paper was to examine the impact of radiation and Marangoni convective boundary conditions on the flow of various ternary hybrid nanofluids in permeable media along mass transpiration. Using similarity transformations, the governing partial differential equations were turned into ordinary differential equations. In the fluid flow, three different shaped nanoparticles were mixed: spherical Silver (Ag), cylindrical SWCNT, and platelet graphene. The following are the important observations:

- The variation in the concentrations of ternary nanoparticles plays a critical influence in thermal performance owing to nanoparticle shape configuration.
- Solid volume fraction increases with decreasing the thickness of the boundary layer.
- Porosity enhances with enhancing the boundary layer thickness in both suction and injection cases, respectively. And mass transpiration in the case of suction, increases with decreasing the velocity, whereas in the case of injection it causes the inverse effect.
- In the temperature/concentration profiles, the porosity, volume fraction and radiation will increase by increasing the concentrations.

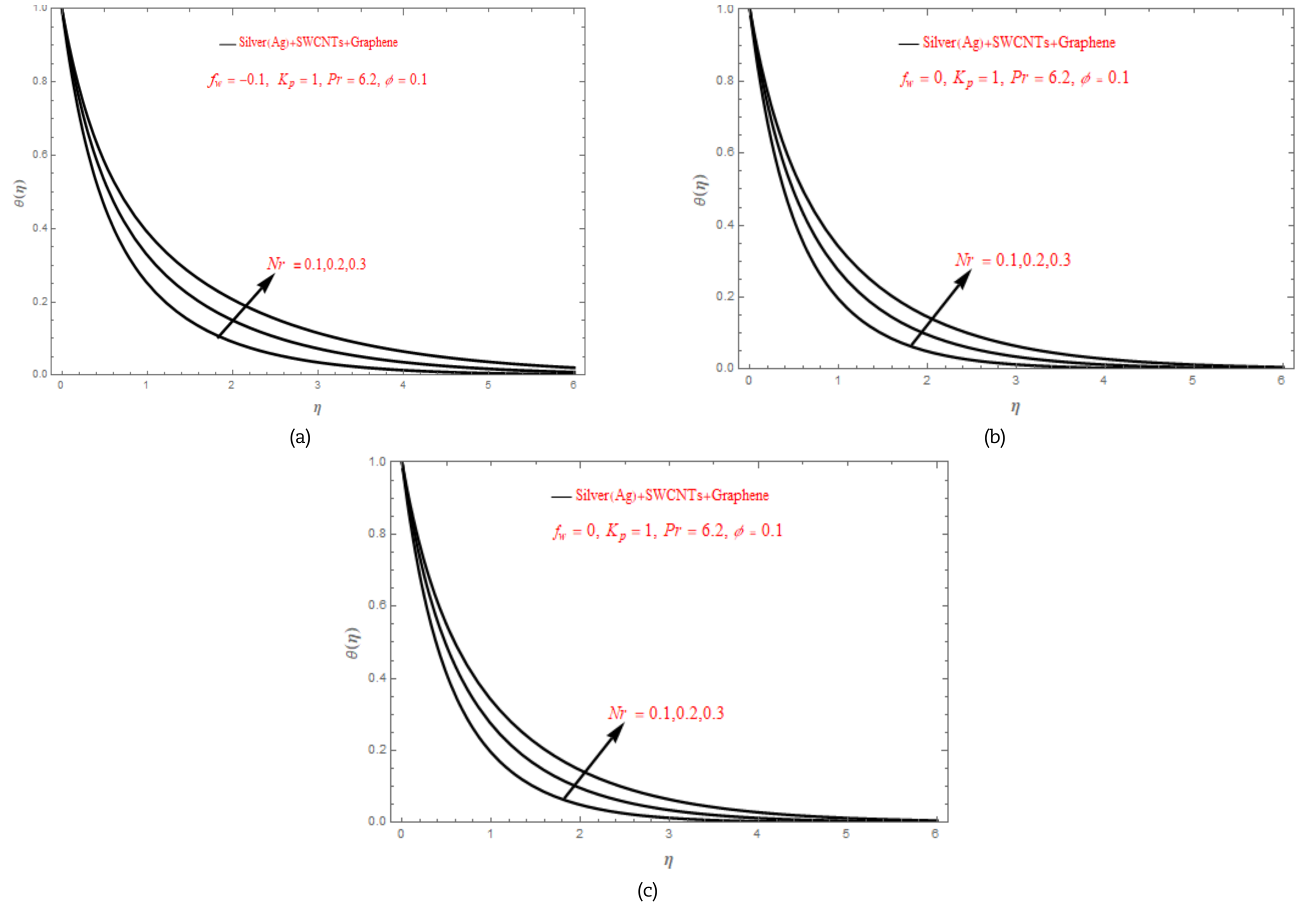

Fig. 7. (a) Temperature profile for variation of radiation with values of f_w =- 0.1 and K_p = 1 (b) Temperature profile for variation of radiation with values of f_w = 0 and K_p = 1 (c) Temperature profile for variation of radiation with values of f_w = 0.1 and K_p = 1.

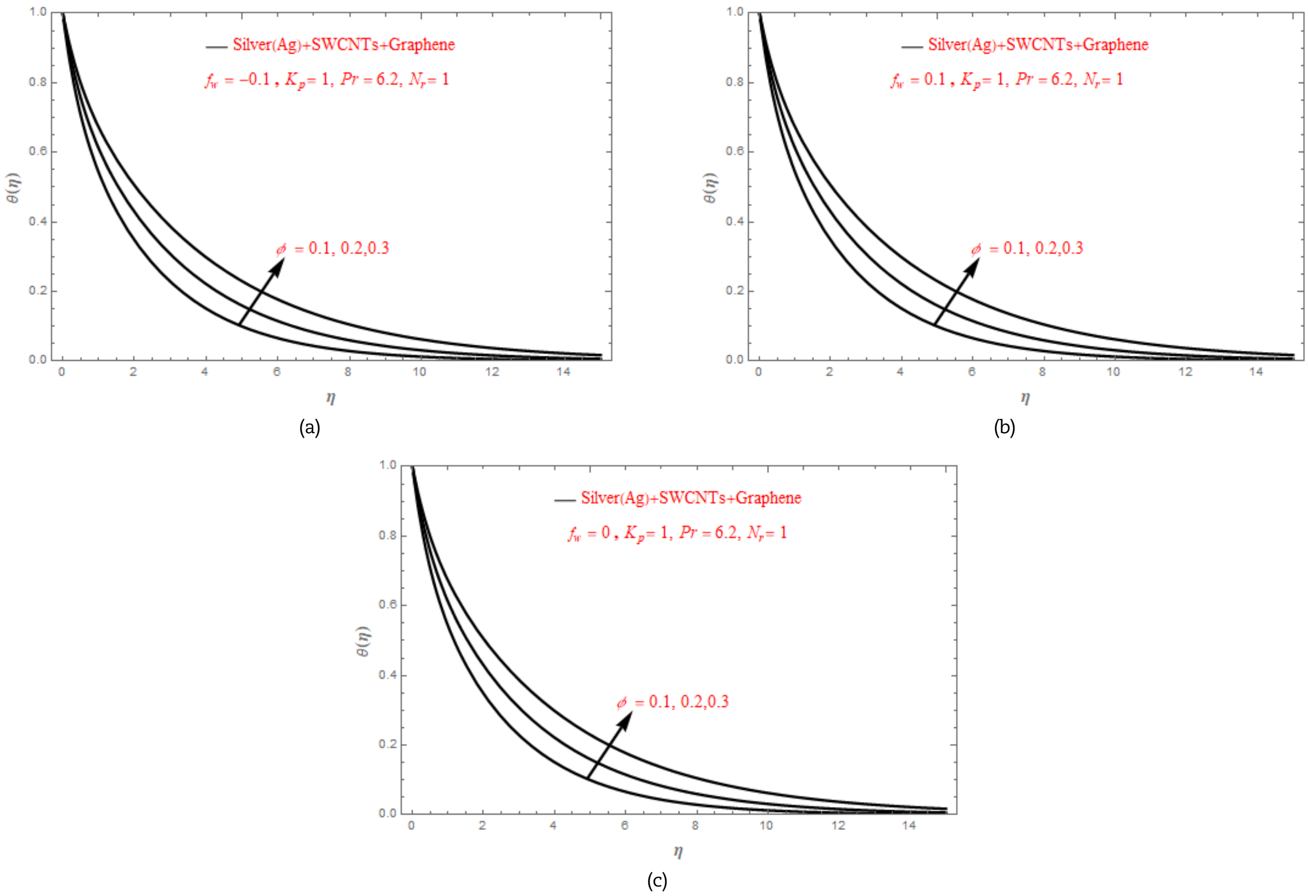

Fig. 8. (a) Temperature distribution for variation of ϕ with values of f_w = -0.1 and K_p = 1 (b) Temperature distribution for variation of ϕ with values of f_w = 0.1. and K_p = 1 (c) Temperature distribution for variation of ϕ with values of f_w = 0. and K_p = 1.

The current work is limited by some previous works:

- We acquired the result of ternary nanofluid flow in porous media by replacing the nanofluid.
- In the absence of MHD, the results of the problem showed that the electrical conductivity of base fluid is so small.

Author Contributions

Methodology, validation, investigation, visualization, T. Maranna; Conceptualization, formal analysis, data curation, writing-original draft preparation, supervision, U.S. Mahabaleshwar; data curation, writing-original draft preparation, writing-review and editing, supervision, M.I. Kopp. All authors have read and agreed to the published version of the paper.

Acknowledgments

We thank two anonymous reviewers for their valuable suggestions and comments. We would also like to thank the editor for his suggestions.

Conflict of Interest

The authors declared no potential conflicts of interest concerning the research, authorship, and publication of this article.

Funding

The authors received no financial support for the research, authorship, and publication of this article.

Data Availability Statements

Data and codes that support the findings of this study are available from the corresponding author upon reasonable request.

Nomenclature

a	Constant	α	Thermal diffusivity [$m^2 s^{-1}$]
C_p	Specific heat [$JK^{-1} Kg^{-1}$]	η	Similarity variable
F	Suction/injection parameter	θ	Temperature similarity variable
K_p	Permeability [$N A^{-1}$]	ψ	Stream function
Nr	Radiation parameter	ϕ	Volume fraction of the nanoparticle
Pr	Prandtl Number	ϕ_1	Volume fraction of the spherical nanoparticle
q_r	Radiative flux [Wm^{-2}]	ϕ_2	Volume fraction of the cylindrical nanoparticle
T	Fluid temperature [K]	ϕ_3	Volume fraction of the platelet nanoparticle
u	Velocity component of x-axis [ms^{-1}]	μ_{tnf}	Dynamic viscosity [$Ns\ m^{-2}$]
v	Velocity component of y-axis [ms^{-1}]	ρ_{tnf}	Effective density [$Kg\ m^{-3}$]
u_w	Surface velocity [ms^{-1}]	υ_{tnf}	Kinematic viscosity [$m^2 s^{-1}$]
tnf	Ternary Nanofluid	σ_0	Equilibrium surface tension
PDEs	Partial Differential Equations	σ	Surface tension [N/m]
ODEs	Ordinary Differential Equations	σ^*	Stefan-Boltzmann constant

References

[1] Shakya, A., Yahya, S.M., Ansari, M.A., Khan, S.A., Role of 1-butanol on critical heat flux enhancement of TiO_2, Al_2O_3, and CuO nanofluids, *Journal of Nanofluids*, 8(7), 2009, 1560-1565.
[2] Crane L.J., Flow past a stretching sheet, *Journal of Applied Mathematics and Physics*, 21, 1970, 645-647.
[3] Wang, C.Y., Fluid flow due to a stretching cylinder, *Physics of Fluids*, 31, 1988, 466-468.
[4] Siddheshwar, P.G., Mahabaleshwar, U.S., Effect of radiation and heat source in MHD flow of a viscoelastic liquid and heat transfer over a stretching sheet, *International Journal of Non-linear Mechanics*, 40(6), 2005, 807-820.
[5] Choi, S.U.S., Eastman, J.A., Enhancing thermal conductivity of the fluids with nanoparticles, Argonne National Lab. (ANL), Argonne IL, United States, 1995.
[6] Napolitano, L.G., Microgravity fluid dynamics, *2nd Levitch Conference*, 1978.
[7] Napolitano, L.G., Marangoni boundary layers, *In: Proceedings of the 3rd European Symposium on Material Science in Space*, Grenoble, ESA SP-142, 1979.
[8] Napolitano, L.G., Surface and buoyancy driven free convection, *Acta Astronautics*, 9, 1982, 199-215.
[9] Mahabaleshwar, U.S., Nagaraju, K.R., Vinay Kumar, P.N., Azese, M.N., Effect of radiation and thermosolutal Marangoni convection in a porous medium with chemical reaction and heat source/sink, *Physics of Fluids*, 32(11), 2020, 113602.
[10] Anush, T., Haung, H.N., Mahabaleshwar, U.S., Two dimensional unsteady stagnations point flow of Casson hybrid nanofluid over a permeable flat surface and heat transfer analysis with radiation, *Journal of the Taiwan Institute of Chemical Engineers*, 127, 2021, 79-91.
[11] Aslani, K.E., Mahabaleshwar, U.S., Singh, J., Sarris, I.E., Combined effect of radiation and inclined MHD flow of a micro polar fluid over a porous stretching/shrinking sheet with mass transpiration, *International Journal of Applied and Computational Mathematics*, 60(7), 2021, 1-21.
[12] Mahabaleshwar, U.S., Vinay Kumar, P.N., Sheremet, M., MHD flow of nanofluid driven by a stretching/shrinking sheet with suction, *Springer Plus*, 5(1), 2016, 1-9.
[13] Mahabaleshwar, U.S., Sneha, K.N., Haung, H.N., An effect of MHD and radiation on CNTs- water based nanofluids due to a stretching sheet in a Newtonian fluid, *Case Studies in Thermal Engineering*, 28(2), 2021, 101462.
[14] Animasuan, I.L., Yook, S.J., Muhammed, T., Mathew, A., Dynamics of ternary hybrid nanofluid subjected to Magnetic flux density and heat source or sink on a convectively heated surface, *Journal of Surfaces and Interfaces of Materials*, 28, 2022, 101654.
[15] Manjunatha, S., Puneeth, V., Gireesh, B.J., Chamkha, A.J., Theoretical study of convective heat transfer in ternary nanofluid flowing past a stretching sheet, *Journal of Applied and Computational Mechanics*, 8, 2022, 1279-1286.
[16] Xuan, Z., Zhai, Y., Mingyan, Ma., Li, Y., Wang, H., Thermo-economic performance and sensitivity analysis of ternary hybrid nanofluids, *Journal of Molecular Liquids*, 323, 2021, 114889.

[17] Sahoo, R.R., Kumar, V., Development of a new correlation to determine the viscosity of ternary hybrid nanofluid, *International Communications in Heat and Mass Transfer*, 111, 2020, 104451.
[18] Sahoo, R.R., Experimental study on the viscosity of hybrid nanofluid and development of a new correlation, *Heat and Mass Transfer*, 56, 2020, 3023-3033.
[19] Magyari, E., Chamka, A.J., Exact analytical results for the thermosolutal MHD Marangoni boundary layers, *International Journal of Thermal Sciences*, 47(7), 2008, 848-8572.
[20] Nanjundappa, C.E., Shivakumar, I.S., Arunkumar, R., Benard-Marangoni ferroconvection with Magnetic field dependent viscosity, *Journal of Magnetism and Magnetic Materials*, 322(15), 2010, 2256-2263.
[21] Manjunatha, S., Kuttan, B.A., Jayanthi, S., Chamkha, A.J., Gireesh, B.J., Heat transfer enhancement in the boundary layer flow of hybrid nanofluids due to variable viscosity and natural convection, *Heliyon*, 5(4), 2019, 01464.
[22] Gupta, G., Rana, P., Comparative study on Rosseland's heat flux on three-dimensional MHD Stagnation-point multiple slip flow of ternary hybrid nanofluid over a stretchable rotating disk, *Mathematics*, 10, 2022, 3342.
[23] Mahabaleshwar, U.S., Vishalakshi, A.B., Anderson, H.I., Hybrid nanofluid flow past a stretching/shrinking sheet with Thermal radiation and mass transpiration, *Chinese Journal of Physics*, 75, 2022, 152-168.
[24] Udawattha, D.S., Narayan, M., Development of a model for predicting the effective thermal conductivity of nanofluids: A reliable approach for nano fluids containing spherical nanoparticlesm *Journal of Nanofluids*, 7(1), 2018, 129-140.
[25] Ekiciler, R., Aydeniz, E., Arsian, K., Effect of shape of nanoparticles on heat transfer and energy generation of nanofluid-jt impingement cooling, *International Journal of Green Energy,* 17(10), 2020, 555-567.
[26] Magyari, E., Chamkha, A.J., Analytical solution for thermosolutal Marangoni convection in the presence of heat and mass generation or consumption, *Heat and Mass Transfer*, 43, 2007, 965-974.
[27] Aly, E.H., Ebaid, A., Exact analysis for the effect of heat transfer on MHD and radiation Marangoni boundary layer nanofluid flow past a surface embedded in a porous medium, *Journal of Molecular Liquid*, 215, 2016, 625-659.
[28] Deb, H.R., Visco-elastic effects on MHD free convection and mass transfer for boundary layer flow with radiation and transpiration, *International Journal Applied Engineering Research,* 12, 2017 11279-11287.
[29] Mahabaleshwar, U.S., Sarris, I.E., Lorenzini, G., Effect of radiation and Navier slip boundary of Walter's liquid B flow over a stretching sheet in a porous media, *International of Heat and Mass transfer*, 127, 2018, 1327-1337.
[30] Vishalakshi, A.B., Maranna, T., Mahabaleshwar, U.S., Laroze, D., An effect of MHD on Non-Newtonian fluid flow over a porous stretching/shrinking sheet with heat transfer*, Applied Science*, 12(10), 2022, 4937.
[31] Maranna, T., Sneha, K.N., Mahabaleshwar, U.S., Sarris, I.E., Karakasidis, T.E., An impact of radiation and MHD Newtonian fluid flow over a stretching/shrinking sheet with CNTs and mass transpiration, *Applied Science*, 12(11), 2022, 5466.
[32] Aly, E.H., Mahabaleshwar, U.S., Anush, T., Usafzai, W.K., Pop, I., Wall jet flow and heat transfer of a hybrid nanofluid subjected to suction/injection with thermal radiation, *Thermal Science and Engineering Progress*, 32, 2022, 101294.
[33] Saleem, S., Animasuan, I.L., Yook, S.J., Al-Mdallal, Q.M., Shah, N.A., Faisal, M., Insight into the motion of water conveying three kinds of nanoparticles on a horizontal surface: significance of thermos-migration and Brownian motion of different nanoparticles, *Surface and Interface Analysis*, 30(7), 2022, 101854.
[34] Sahu, M., Sarkar, J., Steady-state energentic and exergetic performance of single-phase natural circulation loop with hybrid nanofluids, *Journal of Heat Transfer*, 141(8), 2019, 082401.
[35] Nehad, A.S., Animasaun, I.L., Wakif, A., Koriko, O.K., Sivaraj, R., Adegbie, K.S., Abdelmalek, Z., Vaidya, H., Ijirimoye, A.F., Prasad, K.V., Significance of suction and dual stretching on the dynamics of various hybrid nanofluid: comparative analysis between type I and type II models, *Physica Scripta*, 95(9), 2020, 095205.
[36] Takabi, B., Saleh, S., Augmentation of the heat transfer performance of a sinusoidal corrugated enclosure by employing hybrid nanofluid, *Advances in Mechanical Engineering*, 16, 2014, 147059.
[37] Kalidasan, K., Velkennedy, L.R., Kanna, P.R., Laminar natural convection of copper titania/water hybrid nanofluid in an open-ended C- shaped enclosure with an Isothermal block, *Journal of Molecular Liquid*, 246, 2017, 251-258.
[38] Dhanalakshmi, M., Reddy, K.J., Heat and mass transfer effects on MHD free convective flow over a permeable stretching surface with suction, viscous dissipation and heat generation in the presence of chemical reaction, *International Journal of Applied and Engineering Research*, 7, 2018, 5271-5280.

ORCID iD

Thippaiah Maranna https://orcid.org/0000-0001-7059-8632
Ulavathi S. Mahabaleshwar https://orcid.org/0000-0003-1380-6057
Michael I. Kopp https://orcid.org/0000-0001-7457-3272

How to cite this article: Maranna T., Mahabaleshwar U.S., Kopp M.I. An Impact of Marangoni Convection and Radiation on Flow of Ternary Nanofluid in a Porous Medium with Mass Transpiration, *J. Appl. Comput. Mech.*, 9(2), 2023, 487–497. https://doi.org/10.22055/jacm.2022.41405.3748